

## Dimerized and trimerized phases for spin-2 bosons in a one-dimensional optical lattice

Pochung Chen,<sup>1</sup> Zhi-Long Xue,<sup>1</sup> I. P. McCulloch,<sup>2</sup> Ming-Chiang Chung,<sup>3</sup> and S.-K. Yip<sup>4</sup>

<sup>1</sup>*Physics Department, National Tsing Hua University, Hsinchu 30013, Taiwan*

<sup>2</sup>*School of Physical Sciences, The University of Queensland, Brisbane, Queensland 4072, Australia*

<sup>3</sup>*Physics Division, National Center for Theoretical Sciences, Hsinchu 30013, Taiwan*

<sup>4</sup>*Institute of Physics, Academia Sinica, Taipei 11529, Taiwan*

(Received 18 May 2011; published 3 January 2012)

We study the phase diagram for spin-2 bosons loaded in a one-dimensional optical lattice. By using the non-Abelian density matrix renormalization group (DMRG) method we identify three possible phases: ferromagnetic, dimerized, and trimerized phases. We sketch the phase boundaries based on DMRG. We illustrate two methods for identifying the phases. The first method is based on the spin-spin correlation function, while in the second method one observes the excitation gap as a dimerization, or a trimerization superlattice is imposed. The advantage of the second method is that it also can be easily implemented in experiments. By using the scattering lengths in the literature we estimate that <sup>83</sup>Rb, <sup>23</sup>Na, and <sup>87</sup>Rb can be ferromagnetic, dimerized, and trimerized, respectively.

DOI: [10.1103/PhysRevA.85.011601](https://doi.org/10.1103/PhysRevA.85.011601)

PACS number(s): 67.85.Fg, 03.75.Mn, 67.85.Hj

Cold atomic gases have been actively studied in recent years because they offer different possibilities for studying quantum many-body systems [1]. In the very early experiments of a dilute Bose gas in a trap, Bose-Einstein condensation was observed directly [2]. We have also witnessed the realization of the Bose-Hubbard model and the observation of the superfluid-Mott transition [3], a phenomenon theoretically predicted long ago but only observed recently. In this case, the presence of a lattice and the interatomic interaction actually destroy the superfluid, resulting in an “insulating” state. In Ref. [3] and also in the many following experiments, the bosons are spin polarized and so they are effectively spinless. However, Bose-Einstein condensation of bosons with spin degree of freedom has also been realized [4]. Hence it is natural to ask what would be the spin ordering of such bosons in a lattice in the Mott-insulating state, where, even though one is confined to an integral number of particles per site, the spins of the neighboring sites can still interact via virtual tunneling. Indeed, this question is of much theoretical interest, as it can be easily shown that the effective spin Hamiltonians one can realize for spinor bosons loaded in an optical lattice are very different from the Heisenberg-like Hamiltonians that have been much studied in electronic systems [5]. Similarly, a two-component Bose system allows us to realize the XXZ spin-1/2 model [6], which has been discussed considerably in the theoretical literature.

In this Rapid Communication, we consider spin-2 bosons in a one-dimensional lattice. Spin-2 systems are already available and have been experimentally studied [7–10]. The theoretical phase diagram of spin-2 condensates is a function of the scattering lengths  $a_S$  in the spin  $S = 0, 2, 4$  channels [11,12]. It is divided into three regions, which are named ferromagnetic (F), polar (P), and cyclic (C) in Ref. [11]. For spin-2 bosons with one particle per site in a higher dimensional lattice in the insulating phase, it can be easily shown that again the phase diagram is divided into three regions in the mean-field limit, in direct analogy to the Bose-condensed case [13–16] (see also Ref. [17]). In one dimension (1D), however, strong quantum fluctuations are expected to substantially modify the phases. In particular, the polar and cyclic phases are no longer expected

to be stable. These states break rotational symmetry, which implies the existence of linear Goldstone modes, and thus they have diverging quantum fluctuations in 1D.

In this Rapid Communication, we use the non-Abelian density matrix renormalization group (DMRG) method to determine the general phase diagram for one particle per site. This regime is much more stable than multiparticles per site and thus has a much better chance of being realized experimentally. We find three phases, which are ferromagnetic (F), dimerized (D), and trimerized (T) phases. The ferromagnetic state has a macroscopic spin, and has large degeneracies arising from the choice of the spin projections. The dimerized phase has a spontaneously broken lattice symmetry, with the unit cell consisting of two lattice sites. The ground state is a spin singlet, with finite gaps to the first excited states. The trimerized phase is the most intriguing. At a finite size with the total number of sites  $N$  being multiples of 3, the system is gapped with a spin-singlet ground state. The gap, however, approaches zero as  $N \rightarrow \infty$ , resulting in a gapless phase. In this  $N \rightarrow \infty$  limit, there is also *no* broken lattice symmetry. In the following we shall discuss this general phase diagram and present numerical evidence that leads to our claims. We further discuss the expected ground states for some available spin-2 elements and how the dimerized and trimerized phases can be obtained experimentally as well as being tested.

We begin with the Hamiltonian. Assuming only a nearest-neighbor interaction, it is given by  $H = \sum_{i=1}^{N-1} H_{i,i+1}$ , where  $i$ 's denote the sites in increasing order, and  $N$  is the total number of sites.  $H_{i,i+1}$  can be written as

$$H_{i,i+1} = \epsilon_0 P_{0,i,i+1} + \epsilon_2 P_{2,i,i+1} + \epsilon_4 P_{4,i,i+1}, \quad (1)$$

where  $P_{S,i,i+1}$  denotes projection operators for sites  $i$  and  $i+1$  onto a state with total spin  $S$ . Within second-order perturbation theory in the hopping  $t$  between nearest neighbors,  $\epsilon_S = -4t^2/U_S$ , where  $U_S$  is the Hubbard repulsion for two particles with spin  $S$  on the same site.  $U_S$  is proportional to  $a_S$ , the  $s$ -wave scattering length in the spin  $S$  channel. For the one-particle per site to be stable, we then need  $U_S > 0$  for all  $S = 0, 2, 4$ , and hence  $\epsilon_0, \epsilon_2, \epsilon_4 < 0$ . Within DMRG, however,

it is more convenient to explicitly express  $H_{i,i+1}$  in terms of spin-2 operators  $\mathbf{S}_i$ , resulting in

$$H_{i,i+1} = \sum_{n=1}^4 \alpha_n(\epsilon_0, \epsilon_2, \epsilon_4) (\mathbf{S}_i \cdot \mathbf{S}_{i+1})^n, \quad (2)$$

where  $\alpha_1 = -1/3\epsilon_0 - 20/21\epsilon_2 + 1/28\epsilon_4$ ,  $\alpha_2 = -17/180\epsilon_0 - 1/9\epsilon_2 + 1/40\epsilon_4$ ,  $\alpha_3 = +1/45\epsilon_0 + 1/18\epsilon_2 + 1/180\epsilon_4$ , and  $\alpha_4 = +1/180\epsilon_0 + 1/126\epsilon_2 + 1/2520\epsilon_4$  [18–20]. Since it is crucial to identify the total spin for ground and excited states, we use the non-Abelian DMRG [21] which allows us to find the lowest-energy state in different total spin sectors:  $S_{\text{tot}} = 0, 1, 2, 3, 4$ , and  $2N$ . Here we take  $N$  up to 60 with an open-boundary condition (OBC), the number of states is kept at  $m = 400$ , and we perform more than 20 sweeps to ensure the convergence. We note that, although Eq. (2) is more useful for numerical computations, it is more convenient to discuss the physics using Eq. (1), which we shall do below.

Since the phase diagram cannot depend on the overall energy scale, we plot the phase diagram in terms of the variables  $(x_0, x_2, x_4) \equiv (\epsilon_0, \epsilon_2, \epsilon_4)/(\epsilon_0 + \epsilon_2 + \epsilon_4)$ . By definition,  $0 \leq x_{0,2,4} \leq 1$  and  $\sum_i x_i = 1$ . It is therefore convenient to present our results using a ternary phase diagram, where  $x_{0,2,4}$  are depicted as positions in an equilateral triangle. We place the points  $(0, 0, 1)$ ,  $(1, 0, 0)$ , and  $(0, 1, 0)$  at the lower left-hand side, lower right-hand side, and the upper corner of the triangle, respectively. The coordinates  $(x_0, x_2, x_4)$  at a given point within the triangle are to be read off by drawing parallel lines toward the edges and then reading off the intersections. Our main result is as shown in Fig. 1.

To describe and understand the results, we begin by giving the mean-field phase diagram as a useful reference. As mentioned, this can be found in direct analogy with the Bose-condensed case [11,12] (see also Refs. [13, 14,17]). The stability region for each phase is (in the form of Ref. [11]) F :  $\epsilon_2 - \epsilon_4 > 0, (\epsilon_0 - \epsilon_4) + \frac{10}{7}(\epsilon_2 - \epsilon_4) > 0$ , P :  $\epsilon_0 - \epsilon_4 < 0, |\epsilon_0 - \epsilon_4| > \frac{10}{7}|\epsilon_2 - \epsilon_4|$ , and C :  $\epsilon_2 - \epsilon_4 < 0, (\epsilon_0 - \epsilon_4) - \frac{10}{7}(\epsilon_2 - \epsilon_4) > 0$ . The phase boundaries are

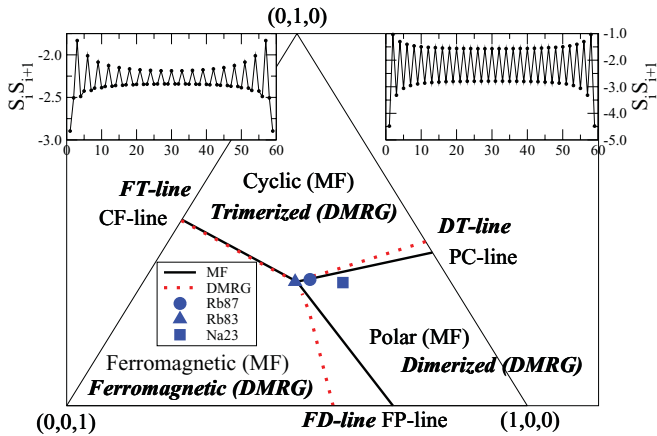


FIG. 1. (Color online) Phase boundaries obtained by MF (black solid lines) and DMRG (red dotted lines). Upper left-hand side: Spin-spin correlation for the  $(0, 1, 0)$  point. Upper right-hand side: Spin-spin correlation for  $^{23}\text{Na}$ . ( $N = 60$ .) The locations of  $^{23}\text{Na}$ ,  $^{83}\text{Rb}$ , and  $^{87}\text{Rb}$  within this parametrization are indicated by the blue square, triangle, and circle, respectively.

plotted as black, solid lines in Fig. 1. F, P, and C occupy, respectively, the lower left-hand side, lower right-hand side, and the upper part of the triangle. Since the mean-field energies of the phases must be linear functionals of  $\epsilon_S$ 's, the phase boundaries are straight lines. They all originate from the point where  $x_0 = x_2 = x_4 = 1/3$ , the center of the triangle, where all three phases are degenerate. The intersection points at the edges are FP  $(17/24, 0, 7/24)$ , PC  $(10/17, 7/17, 0)$ , and CF  $(0, 1/2, 1/2)$ .

Now we proceed to describe our phase diagram based on DMRG. Before we discuss each phase in detail, we summarize our finding as follows: The polar phase is replaced by the dimerized phase, while the cyclic phase is replaced by the trimerized phase. The FD and DT lines (no longer straight lines) are shifted away from the FP and PC lines but the FT line remains indistinguishable with the CF line. We note that, when  $x_2 = x_4 = 0$  and  $x_0 = 1$ , the existence of the gapped dimer order can be proven rigorously [22]. When  $x_2 = x_4$  the system has an enlarged  $\text{SO}(5)$  symmetry. It has been argued [23] that the ground state is also dimerized as long as  $x_0 > 1/3$ .

The phase diagram is easiest to understand for the lower left-hand region where  $x_4 > x_{0,2}$ . It is clear that the system would like to acquire the largest possible total spin. For  $N$  sites, the total spin is  $S = 2N$ . For this state, any two neighboring sites have a total spin 4 and the bond energy is  $\epsilon_4$ , the smallest possible value. The ground state is thus  $4N + 1$ -fold degenerate. From our DMRG calculations we find that the stability region for this state F actually extends slightly beyond  $x_4 > x_0$ .

For the rest of the phase diagram, it is more convenient to first consider finite  $N$ . Later, we shall mention how these pictures are modified as  $N \rightarrow \infty$ .

We find that the lower right-hand region of the triangle is occupied by the dimerized phase, where the unit cell is doubled, and the system is in a nondegenerate singlet state. In upper right-hand inset of Fig. 1 we provide an example for the spin-spin correlation function between neighboring sites, where the parameters of  $^{23}\text{Na}$  are used. The correlation function clearly shows a “strong-weak” dimer pattern. This phase is in direct analogy with the spin-1 case [24]. The ground state for  $N = 2p$  sites can be most simply understood by first considering the case of  $x_0 \approx 1$  and imposing an artificial dimerization superlattice, where alternate bonds are weakened by a factor  $0 \leq \lambda_2 \leq 1$  (i.e.,  $H_{2i,2i+1} \rightarrow \lambda_2 H_{2i,2i+1}$ ). When  $\lambda_2 = 0$ , the system breaks into  $N/2$  subsystems, each consisting of only two interacting sites. For  $x_0 \approx 1$ , these two sites form a singlet with a finite gap to the first excited state(s), and the system is maximally dimerized. As one increases  $\lambda_2$ , one expects that the gap should decrease gradually. In Fig. 2(a) (left-hand panel) we plot the gap for the first two excited states as a function of  $0 \leq \lambda_2 \leq 1$ . We observe that the gap decreases monotonically with increasing  $\lambda_2$  but never vanishes, indicating the original ground state at  $\lambda_2 = 1$  is adiabatically connected with that at  $\lambda_2 = 0$  and hence it is indeed dimerized.

Next we focus on the upper corner of the triangle, where we find the trimerized phase. For  $N = 3p$ , we find that the ground state is a spin singlet, with a finite gap to the first excited state. In upper left-hand inset of Fig. 1 we provide an example for the spin-spin correlation function between neighboring sites for

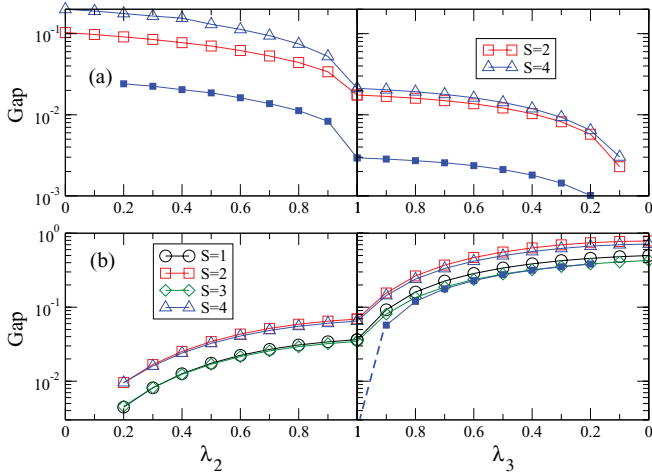


FIG. 2. (Color online) Excitation gaps to first few excited states with total spin  $S$  for  $^{23}\text{Na}$  (upper plot) and the  $(0,1,0)$  point (lower plot) when a dimerization (trimerization) superlattice of strength  $\lambda_2(\lambda_3)$  is imposed. Open symbols:  $N = 60$ ; solid symbols: lowest excited state for  $N \rightarrow \infty$ .

the case of  $x_2 = 1$ . It shows a “strong-strong-weak” pattern, indicating that the ground state is trimerized. To get a physical picture of this trimerized phase, it is helpful to consider a three-spin system in the limit where  $x_2 \approx 1$ . For two interacting spins, the ground state is fivefold degenerate, belonging to  $S = 2$ . For three spins (say 1, 2, and 3), however, the ground state is a unique singlet: The total spin of any two spins can be 0, 1, 2, 3, 4, and only the spin-2 combination can be added to the third spin to form a singlet. By the same argument, this state is an eigenstate for both the operators  $H_{12}$  and  $H_{23}$ , with eigenvalues  $\epsilon_2$ . Hence the system has a total energy  $2\epsilon_2$ , the lowest possible value. For a system with  $N = 3p$  sites, it is again helpful to impose a trimerization superlattice, where one out of every three bonds are weakened by a  $\lambda_3$  factor ( $H_{3i,3i+1} \rightarrow \lambda_3 H_{3i,3i+1}$ ,  $0 \leq \lambda_3 \leq 1$ ). For  $\lambda_3 \rightarrow 0$ , the system break up into  $N/3$  subsystems, each one with a singlet ground state as just described and the whole system is maximally trimerized. The system at  $\lambda_3 = 0$  is hence gapped, and it is stable toward increasing  $\lambda_3$  from 0. In Fig. 2(b) (right-hand panel) we show the gap as a function of  $\lambda_3$ . We find that the gap decreases monotonically with  $\lambda_3$  but always remains finite, indicating that the ground state is adiabatically connected to the trimerized ground state of the  $\lambda_3 = 0$  limit.

It is also instructive to study the behavior of the gap when an incorrect superlattice is imposed. Consider a state in the dimerized (trimerized) phase. If one imposes a trimerization (dimerization) superlattice with strength  $\lambda_3(\lambda_2)$ , the system will be converted into a trimerized (dimerized) phase as  $\lambda_3(\lambda_2) \rightarrow 0$ . As a result, one expects that there is a qualitative change in the ground state when  $\lambda_3(\lambda_2)$  is varied from 1 to 0, and the gap must vanish at a transition point. In Fig. 2 we also plot the gap as the function of  $\lambda_{2,3}$ , when such an incorrect superlattice is imposed. We observe that the gap does vanish before  $\lambda_{2,3}$  reaches zero, which provides an alternative confirmation for the nature of the phases.

Now we consider  $N \rightarrow \infty$ . For the dimerized phase, our description above remains valid, except that the magnitude of

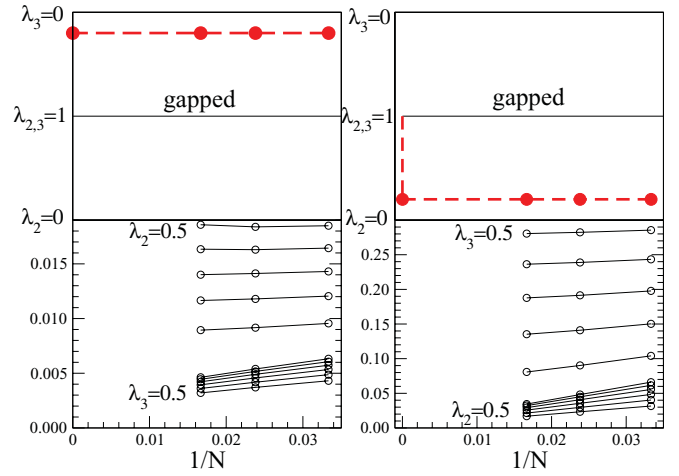


FIG. 3. (Color online) “Phase diagram” (top panels) and energy gaps (lower panels) as a function of  $N$  and  $\lambda_{2,3}$ . The red dotted lines indicate where the system becomes gapless. Left-hand column: Parameters according to  $^{23}\text{Na}$ . Right-hand column: The point  $(0,1,0)$ .

the gap becomes smaller (see Fig. 2, solid symbols). That is, the system remains gapped, unless a sufficiently strong “incorrect” superlattice is imposed. For the trimerized phase, however, the situation is slightly different. Without any superlattice, the gap vanishes as  $1/N$  as  $N \rightarrow \infty$ . That is, the system becomes gapless, and the spin-spin correlation function  $\langle \mathbf{S}_i \cdot \mathbf{S}_j \rangle$  decays algebraically [25]. Also, the trimer order parameter defined by the appropriate sums and differences of the neighboring spin-spin correlation vanishes as  $N \rightarrow \infty$  (not shown) [26]. Nevertheless, for any finite  $\lambda_3$ , we find that the gap remains finite as  $N \rightarrow \infty$ . The gapped region as a function of  $\lambda_{2,3}$  and  $1/N$ , as well as the gap dependence, are shown in Fig. 3.

It is natural to ask what are the expected phases of some of the available spin-2 elements. Using scattering lengths available in the literature [27], we find that  $^{83}\text{Rb}$  and  $^{23}\text{Na}$  should be in the ferromagnetic and dimerized state, respectively. For  $^{87}\text{Rb}$ , however, the spin-spin correlation only shows a very weak trimerlike pattern (not shown). We hence resort to use the method of imposing superlattices. We impose both trimerization and dimerization superlattices and calculate the gap as a function of  $\lambda_{2,3}$ . We find that the gap monotonically increases under the trimerization superlattice but decreases to zero under the dimerization superlattice. This strongly suggests that the  $^{83}\text{Rb}$  is indeed in a trimerized phase.

Spin-2 bosons in a 1D insulating lattice have been studied theoretically before in Ref. [28]. Our results differ near the center and the upper corner. We do not find nematic and cyclic phases to be stable and the trimerized phase in the upper corner was not discussed in their paper.

Lastly, we discuss how our picture of the dimerized and trimerized state can be tested experimentally. There have now been many discussions on how to detect spin ordering for atomic gases in optical lattices [29,30]. We here, however, would like to point out a simple scheme that is particularly suitable for our states that is based on the adiabatic

deformation of the Hamiltonian by imposing superlattices as discussed above. Superlattices can be created easily [31], and actually have been utilized already for the preparation and detection of certain spin-ordering states [32]. In our scheme, by applying an optical potential with two or three lattice spacings and changing the laser intensity for this optical potential, one can tune the parameter  $\lambda_{2,3}$  defined above since the tunneling amplitude  $t$  decreases with increasing potential barrier. A trimerized (dimerized) state is then characterized by a monotonic increase of the gap as a function of  $\lambda_3$  ( $\lambda_2$ ) and the gap closing before  $\lambda_2$  ( $\lambda_3$ ) reaches zero. Furthermore, by reversing the above argument, a trimerization (dimerization) superlattice also can allow us to prepare the trimerized (dimerized) state by first preparing the corresponding system with  $\lambda_{3,2} = 0$  and then gradually increasing it until it reaches 1.

In summary, we have studied the phase diagram of spin-2 bosons in 1D optical lattice using non-Abelian DMRG. We identify three possible phases, namely, ferromagnetic, dimerized, and trimerized, where the trimerized phase was not proposed in the literature. We demonstrate that by imposing proper superlattices and observing the excitation gap, the phase of interest can be identified or prepared based on the adiabatic connection of the ground state. Such a procedure can be implemented in cold-atom experiments and provide a simple scheme to test the phase diagram experimentally.

We acknowledge inspiring conversations with M. A. Cazalilla, and thank H.-H. Tu for pointing out Ref. [23] to us. This research was supported by the NSC and NCTS of Taiwan. Ian McCulloch acknowledges financial support from the Australian Research Council (project DP1092513).

- 
- [1] I. Bloch, J. Dalibard, and W. Zwerger, *Rev. Mod. Phys.* **80**, 885 (2008).
- [2] M. H. Anderson *et al.*, *Science* **269**, 98 (1995); C. C. Bradley, C. A. Sackett, J. J. Tollett, and R.G. Hulet, *Phys. Rev. Lett.* **75**, 1687 (1995); K. B. Davis *et al.*, *ibid.* **75**, 3969 (1995).
- [3] M. Greiner *et al.*, *Nature (London)* **415**, 39 (2002).
- [4] J. Stenger *et al.*, *Nature (London)* **396**, 345 (1998); M.-S. Chang *et al.*, *Phys. Rev. Lett.* **92**, 140403 (2004); *Nat. Phys.* **1**, 111 (2005).
- [5] S.-K. Yip, *Phys. Rev. Lett.* **90**, 250402 (2003); A. Imambekov, M. Lukin, and E. Demler, *Phys. Rev. A* **68**, 063602 (2003).
- [6] A. B. Kuklov and B. V. Svistunov, *Phys. Rev. Lett.* **90**, 100401 (2003); E. Altman *et al.*, *New J. Phys.* **5**, 113 (2003).
- [7] H. Schmaljohann *et al.*, *Phys. Rev. Lett.* **92**, 040402 (2004).
- [8] T. Kuwamoto, K. Araki, T. Eno, and T. Hirano, *Phys. Rev. A* **69**, 063604 (2004).
- [9] A. Widera *et al.*, *New J. Phys.* **8**, 152 (2006).
- [10] S. Tojo *et al.*, *Phys. Rev. A* **80**, 042704 (2009).
- [11] C. V. Ciobanu, S.-K. Yip, and T.-L. Ho, *Phys. Rev. A* **61**, 033607 (2000).
- [12] M. Koashi and M. Ueda, *Phys. Rev. Lett.* **84**, 1066 (2000).
- [13] F. Zhou and G. W. Semenoff, *Phys. Rev. Lett.* **97**, 180411 (2006).
- [14] R. Barnett, A. Turner, and E. Demler, *Phys. Rev. Lett.* **97**, 180412 (2006).
- [15] The polar phase is also called the nematic phase [13,14], whereas the cyclic phase is also named the tetrahedral state due to its symmetries [14,16].
- [16] S.-K. Yip, *Phys. Rev. A* **75**, 023625 (2007).
- [17] J. L. Song, G. W. Semenoff, and F. Zhou, *Phys. Rev. Lett.* **98**, 160408 (2007); A. M. Turner, R. Barnett, E. Demler, and A. Vishwanath, *ibid.* **98**, 190404 (2007).
- [18] There are a number of recent papers on 1D spin-2 Hamiltonians, e.g., Ref. [19], but their parameter regimes are rather different from the one discussed here, i.e.,  $\epsilon_0, \epsilon_2, \epsilon_4 < 0$ .
- [19] J. Zang, H. C. Jiang, Z. Y. Weng, and S. C. Zhang, *Phys. Rev. B* **81**, 224430 (2010); H.-C. Jiang, S. Rachel, Z. Y. Weng, S. C. Zhang, and Z. Wang, *ibid.* **82**, 220403 (2010).
- [20] We assumed that the magnetic field is sufficiently well screened so that the quadratic Zeeman effect can be ignored. For discussions of its effect in a higher dimensional lattice, see, e.g., M.-C. Chung and S.-K. Yip, *Phys. Rev. A* **80**, 053615 (2009); M. Snoek, J. L. Song, and F. Zhou, *ibid.* **80**, 053618 (2009).
- [21] I. P. McCulloch and M. Gulacsi, *Europhys. Lett.* **57**, 852 (2002); P. McCulloch, *J. Stat. Mech.: Theor. Exp.* (2007) P10014.
- [22] I. Affleck, *J. Phys. Condens. Matter* **2**, 405 (1990).
- [23] H.-H. Tu, G.-M. Zhang, and T. Xiang, *Phys. Rev. B* **78**, 094404 (2008).
- [24] M. Rizzi, D. Rossini, G. DeChiara, S. Montangero, and R. Fazio, *Phys. Rev. Lett.* **95**, 240404 (2005); K. Harada, N. Kawashima, and M. Troyer, *J. Phys. Soc. Jpn.* **76**, 013703 (2007), and references therein.
- [25] See Supplemental Material at <http://link.aps.org/supplemental/10.1103/PhysRevA.85.011601> for the plots of spin-spin correlation functions  $\langle \mathbf{S}_i \cdot \mathbf{S}_j \rangle$ .
- [26] Our trimerized state thus has some strong similarities to the trimerized state found for the spin-1 chain [G. Fáth and J. Solyom, *Phys. Rev. B* **47**, 872 (1993); C. Itoi and M.-H. Kato, *ibid.* **55**, 8295 (1997); A. Läuchli, G. Schmid, and S. Trebst, *ibid.* **74**, 144426 (2006)]. We note also that in the parameter range where this trimerized phase is stable, three spin-1 particles also form a unique spin singlet. We remark, however, here that the parameters needed to realize this spin-1 trimerized phase are quite opposite to those which can be obtained for spin-1 bosons [5].
- [27] For  $^{83}\text{Rb}$ ,  $^{87}\text{Rb}$  and  $^{23}\text{Na}$ , we used the scattering lengths in Ref. [11] provided originally by J. Burke and C. Greene.
- [28] K. Eckert *et al.*, *New J. Phys.* **9**, 133 (2007).
- [29] G. K. Brennen, A. Micheli, and P. Zoller, *New J. Phys.* **9**, 138 (2007).
- [30] K. Eckert, L. Zawitkowski, A. Sanpera, M. Lewenstein, and E. S. Polzik, *Phys. Rev. Lett.* **98**, 100404 (2007); I. de Vega, J. I. Cirac, and D. Porras, *Phys. Rev. A* **77**, 051804(R) (2008).
- [31] S. Peil *et al.*, *Phys. Rev. A* **67**, 051603 (2003).
- [32] S. Trotzky, Y. A. Chen, U. Schnorrberger, P. Cheinet, and I. Bloch, *Phys. Rev. Lett.* **105**, 265303 (2010).